Single-electron quantum dot in Si/SiGe with integrated charge sensing

C. B. Simmons,[a] Madhu Thalakulam, Nakul Shaji, Levente J. Klein, Hua Qin, R. H. Blick, D. E. Savage, M. G. Lagally, S. N. Coppersmith, and M. A. Eriksson[b]
University of Wisconsin-Madison, Madison, Wisconsin 53706, USA

(Received 18 October 2007; accepted 1 November 2007; published online 20 November 2007)

Single-electron occupation is an essential component to the measurement and manipulation of spin in quantum dots, capabilities that are important for quantum information processing. Si/SiGe is of interest for semiconductor spin qubits, but single-electron quantum dots have not yet been achieved in this system. We report the fabrication and measurement of a top-gated quantum dot occupied by a single electron in a Si/SiGe heterostructure. Transport through the quantum dot is directly correlated with charge sensing from an integrated quantum point contact, and this charge sensing is used to confirm single-electron occupancy in the quantum dot. © *2007 American Institute of Physics*. [DOI: 10.1063/1.2816331]

Semiconductor quantum dots provide highly tunable structures for trapping and manipulating individual electrons,[1,2] with significant potential for integration and scaling, and therefore are promising candidates as qubits for quantum computation.[3–6] Because silicon has small spin-orbit coupling and an abundant isotope with zero nuclear spin, electron spins in silicon quantum dots have been predicted to have extremely long coherence times,[7,8] a large advantage for spin-based quantum computing and for spintronics applications. These features have motivated efforts to develop quantum dots in silicon using a wide variety of confinement techniques.[9–18]

Here, we report the achievement of a single-electron quantum dot in a Si/SiGe modulation-doped heterostructure, in which an integrated charge-sensing quantum point contact[11,19–23] is used to monitor electron transitions in and out of the dot and to verify the electron number. Analogous single-electron quantum dots in GaAs/AlGaAs heterostructures have been used to form spin qubits–quantum dots with spin states that can be manipulated and measured.[24–27]

To achieve single-electron quantum dots in Si/SiGe heterostructures, one must overcome complications that do not arise in GaAs/AlGaAs heterostructures, including (1) smaller Schottky barriers, leading to difficulty in the fabrication of low-leakage gates, (2) the need to implement strain management in Si/SiGe heterostructures, leading to disorder in the form of dislocations, mosaic tilt, and surface roughness, and (3) the larger effective mass of carriers in Si compared to GaAs, which decreases the tunneling rate through otherwise equivalent barriers to the leads. Further more, mobility in Si/SiGe is typically smaller than in III-V systems. Our work builds on much recent progress in overcoming many of these issues in Si/SiGe, including the fabrication of gated quantum dots,[10–14] the observation of the Kondo and Fano effects in such a dot,[15] and the demonstration of transport through spin channels in Si/SiGe double dots.[28]

The quantum dot used in this work was formed in a two-dimensional electron gas (2DEG) located 60 nm below the surface in a Si/SiGe heterostructure containing a Si quantum well. Details of the sample can be found in reference Ref. 28. The sample was illuminated for 20 s while at a temperature of 4.2 K at the beginning of the experiment before cooling the dilution refrigerator to base temperature, in order to decrease the resistance of the Ohmic contacts. The results we report below depend critically on the ability to apply large gate voltages without causing leakage currents. The quantum dot was formed on a mesa 10 μm wide by 20 μm long. The Schottky gates were formed by Pd deposition immediately following the removal of the native oxide by brief immersion in hydrofluoric acid. The resulting Schottky gates supported applied voltages as large as −3.25 V relative to the electron gas.

A scanning electron micrograph of the top-gate design is shown in Fig. 1(a). Negative voltages applied to the top gates deplete the underlying electron gas, forming both a single quantum dot defined by gates top (T), left (L), right (R), and the plunger gate (G), and an integrated charge-sensing quantum point contact (QPC) formed by the charge sensor gate (CS) and gate R. Ohmic contacts to the 2DEG (shown schematically on the micrograph by superimposed white squares) were fabricated by the evaporation of a Au:Sb (1%) alloy with subsequent annealing at 550 °C. A dc bias voltage across the top pair or the right pair of these Ohmic contacts causes current to flow through the quantum dot (I_{dot}) or

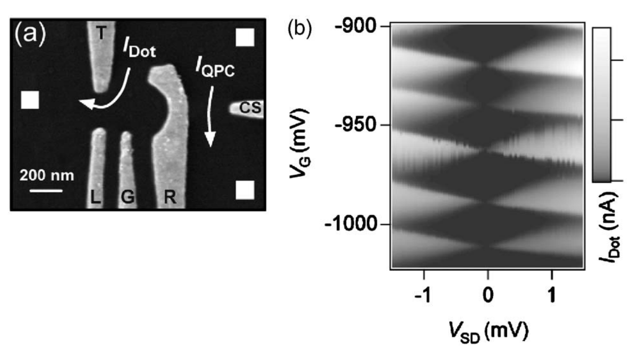

FIG. 1. (a) Scanning electron micrograph of a device with a design identical to the one used in this experiment. Ohmic contact positions are indicated schematically as white squares, and the two current paths, through the dot and through the quantum point contact, are indicated schematically by white arrows. (b) Gray scale plot of the current through the dot as a function of the applied voltage across the dot and the gate voltage V_G. The data were acquired by sweeping V_G from more negative to less negative voltage for each value of V_{SD}.

[a]Electronic mail: cbsimmons@wisc.edu.
[b]Electronic mail: maeriksson@wisc.edu.

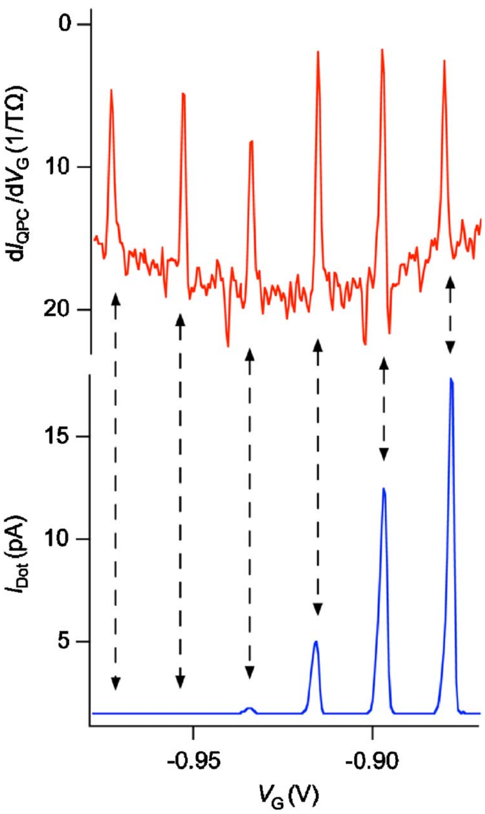

FIG. 2. (Color online) (top) The derivative of the quantum point contact current with respect to the gate voltage dI_{QPC}/dV_G as a function of the gate voltage V_G. The peaks correspond to changes in the number of electrons in the dot. (bottom) The current through the quantum dot as a function of the gate voltage V_G. The peaks in the two curves are well aligned, indicating that the charge-sensing quantum point contact and the Coulomb blockade peaks in transport through the dot correspond to the same quantum dot charging phenomena.

through the QPC (I_{QPC}), respectively. Throughout this paper, the voltage on gate G (V_G) is used to control the number of electrons in the dot, and for the data presented here, the measured electron temperature during the experiment was 300 ± 20 mK.

Figure 1(b) shows a Coulomb diamond plot of the source-drain current as a function of V_G and the source-drain bias (V_{SD}). Based on the electron counting discussed below, we estimate that the electron number in the regime of Fig. 1(b) is approximately 30. As V_G is made more negative, electrons are pushed off the dot one by one. However, more negative V_G also increases the potential barriers between the dot and the source and drain reservoirs, reducing the tunnel coupling between the leads and the dot. This reduced tunnel coupling is visible in Fig. 2(bottom), where the Coulomb peaks decrease in height as V_G is made more negative, until they are below the noise floor of the current measurement, which was 70 fA for the data presented here. At this point, no further transitions in electron number can be monitored using direct current through the dot, and the introduction of a charge-sensing technique using the coupled QPC is essential. It is interesting to note that the larger effective mass in Si ($0.19m_e$) compared with GaAs ($0.067m_e$) decreases the transparency of the tunnel barriers in Si as opposed to GaAs for the same electrostatic barrier shape and height. This may be one of the reasons that past measurements of Coulomb blockade in Si/SiGe have shown a relatively small number of Coulomb peaks.[15] For this reason, we focus in this paper on charge sensing to confirm single-electron occupation.

Applying a negative voltage to gate CS, in combination with the effect of gate R, forms a QPC in close proximity to the quantum dot. By precisely tuning the gate voltage V_{CS}, the conductance of the QPC can be fixed on a steep transition in the pinch-off curve. In this configuration, the QPC functions as a sensitive electrometer for the neighboring quantum dot, because changes in the electron occupation of the dot result in measurable shifts in the QPC pinch-off curve. Numerically differentiating I_{QPC} with respect to V_G turns these discrete shifts into peaks, and such a differentiated curve is plotted in Fig. 2(top). The horizontal axes for the two plots are identical, and the data for each plot were acquired sequentially. There is a clear correspondence between the peaks in the two curves, demonstrating that the QPC functions as a reliable detector of charge transitions in the quantum dot. Importantly, this sensitivity is preserved even when transport through the dot is not measurable, as shown in Fig. 2.

The QPC is most sensitive to charge transitions in the quantum dot when its conductance varies rapidly as a function of gate voltage, and hence also as a function of the charge on the dot. However, changing V_G to remove electrons from the dot also changes the potential of the coupled QPC. The result is that, for a particular value of V_{CS}, there is a finite range over which V_G can vary for which the QPC is sensitive to charge transitions on the dot. Outside this range, the slope of the QPC conductance, which determines the sensitivity to charge transitions in the quantum dot, is too small to allow charge sensing of single electrons. In our system, transitions cannot be detected when dI_{QPC}/dV_G is below $1\ \mathrm{T}\Omega^{-1}$. This provides an effective operational range of approximately 300 mV in V_G. When the dot contains of the order of 30 electrons, this range is large enough to observe many charge transitions in the dot, because the spacing between the transitions is relatively small ($\sim$22 mV). In the few electron regime, however, the spacing between transitions is larger and this range is not sufficient to observe more than three transitions with confidence. Nonetheless, a large dynamic range can still be obtained by compensating the effect of V_G on the QPC by changing V_{CS} in the opposite sense, keeping the QPC in the most sensitive operating point.

An example of this type of compensation is shown in Fig. 3(a). The voltage on gate G is swept through a range much larger than that corresponding to the sensitive region of the QPC. By changing V_{CS}, high sensitivity is maintained across the entire range of V_G, so that many charge transitions can be monitored on a single image plot. These charge transitions appear as the dark vertical lines in Fig. 3(a). The spacing in gate voltage between the peaks is not uniform, as is expected for a dot with very few electrons. The dot is empty of electrons for the most negative values of V_G, as indicated by the absence of dark lines on the left half of the figure. A rigid shift was applied to each horizontal line scan in Fig. 3(a) to remove two effects. First, before the shift is applied, the cross capacitance between gate CS and the quantum dot causes the vertical lines in Fig. 3(a) to slope to more negative V_G for less negative V_{CS} with a lever arm of 26%. In addition, random charge fluctuations cause shifts from line scan to line scan with a rms magnitude of 3.9 mV, which can be compared to the average spacing of 62.1 mV between the peaks.

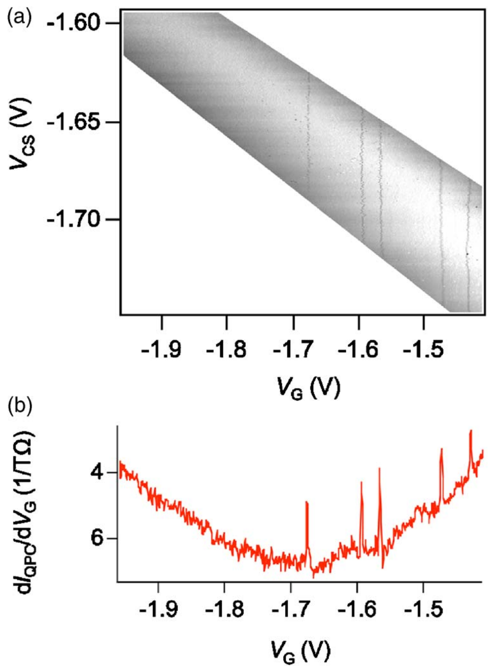

FIG. 3. (Color online) (a) Gray scale plot of the current through the charge-sensing quantum point contact. The dark vertical lines correspond to changes in the quantum dot electron occupation. No further transitions occur for $V_G < -1.68$ V, indicating that the quantum dot is empty of electrons in this regime. (b) An average of seven linecuts taken diagonally down the sensitive slice in part (a). The sharp peaks correspond to changes in the electron occupation of the dot.

Figure 3(b) shows an average of seven diagonal linecuts taken parallel to the sensitive slice in Fig. 3(a). The charge transitions appear as five sharp peaks, corresponding to the removal of the last five electrons from the dot. The sequence of peaks terminates at $V_G = -1.68$ V, indicating that beyond this value of the gate voltage the dot is empty of electrons. It is possible to then reduce the magnitude of V_G, refilling the dot with a known number of electrons starting from zero, something we have done many times over the course of the measurements reported here.

The authors thank Lisa McGuire, Mark Friesen, and Robert Joynt for helpful discussions. This work was supported by NSA and ARO under Contract No. W911NF-04-1-0389, by NSF under Grant Nos. DMR-0325634 and DMR-0520527, and by DOE under Grant No. DE-FG02-03ER46028.

[1]L. P. Kouwenhoven, T. H. Oosterkamp, M. W. S. Danoesastro, M. Eto, D. G. Austing, T. Honda, and S. Tarucha, Science **278**, 1788 (1997).
[2]L. P. Kouwenhoven, C. M. Marcus, P. L. McEuen, S. Tarucha, R. M. Westervelt, and N. S. Wingreen, in *Mesoscopic Electron Transport*, edited by L. L. Sohn, L. P. Kouwenhoven, and G. Schön (Kluwer, Dordrecht, 1997), Vol. 345, p. 105.
[3]D. Loss and D. P. DiVincenzo, Phys. Rev. A **57**, 120 (1998).
[4]B. E. Kane, Nature (London) **393**, 133 (1998).
[5]M. Friesen, P. Rugheimer, D. E. Savage, M. G. Lagally, D. W. van der Weide, R. Joynt, and M. A. Eriksson, Phys. Rev. B **67**, 121301 (2003).
[6]X. D. Hu, B. Koiller, and S. D. Sarma, Phys. Rev. B **71**, 235332 (2005).
[7]R. de Sousa and S. Das Sarma, Phys. Rev. B **68**, 115322 (2003).
[8]C. Tahan, M. Friesen, and R. Joynt, Phys. Rev. B **66**, 035314 (2002).
[9]L. P. Rokhinson, L. J. Guo, S. Y. Chou, and D. C. Tsui, Phys. Rev. B **63**, 035321 (2001).
[10]L. J. Klein, K. A. Slinker, J. L. Truitt, S. Goswami, K. L. M. Lewis, S. N. Coppersmith, D. W. van der Weide, M. Friesen, R. H. Blick, D. E. Savage, M. G. Lagally, C. Tahan, R. Joynt, M. A. Eriksson, J. O. Chu, J. A. Ott, and P. M. Mooney, Appl. Phys. Lett. **84**, 4047 (2004).
[11]M. R. Sakr, H. W. Jiang, E. Yablonovitch, and E. T. Croke, Appl. Phys. Lett. **87**, 223104 (2005).
[12]K. A. Slinker, K. L. M. Lewis, C. C. Haselby, S. Goswami, L. J. Klein, J. O. Chu, S. N. Coppersmith, R. Joynt, R. H. Blick, M. Friesen, and M. A. Eriksson, New J. Phys. **7**, 246 (2005).
[13]L. J. Klein, K. L. M. Lewis, K. A. Slinker, S. Goswami, D. W. van der Weide, R. H. Blick, P. M. Mooney, J. O. Chu, S. N. Coppersmith, M. Friesen, and M. A. Eriksson, J. Appl. Phys. **99**, 023509 (2006).
[14]T. Berer, D. Pachinger, G. Pillwein, M. Muhlberger, H. Lichtenberger, G. Brunthaler, and F. Schaffler, Appl. Phys. Lett. **88**, 162112 (2006).
[15]L. J. Klein, D. E. Savage, and M. A. Eriksson, Appl. Phys. Lett. **90**, 033103 (2007).
[16]H. W. Liu, T. Fujisawa, Y. Ono, H. Inokawa, A. Fujiwara, K. Takashina, and Y. Hirayama (http://arxiv.org/abs/0707.3513).
[17]J. Gorman, D. G. Hasko, and D. A. Williams, Phys. Rev. Lett. **95**, 090502 (2005).
[18]S. J. Angus, A. J. Ferguson, A. S. Dzurak, and R. G. Clark, Nano Lett. **7**, 2051 (2007).
[19]M. Field, C. G. Smith, M. Pepper, D. A. Ritchie, J. E. F. Frost, G. A. C. Jones, and D. G. Hasko, Phys. Rev. Lett. **70**, 1311 (1993).
[20]E. Buks, R. Schuster, M. Heiblum, D. Mahalu, and V. Umansky, Nature (London) **391**, 871 (1998).
[21]J. M. Elzerman, R. Hanson, J. S. Greidanus, L. H. W. van Beveren, S. De Franceschi, L. M. K. Vandersypen, S. Tarucha, and L. P. Kouwenhoven, Phys. Rev. B **67**, 161308 (2003).
[22]T. Fujisawa, T. Hayashi, R. Tomita, and Y. Hirayama, Science **312**, 1634 (2006).
[23]Y. Hu, H. O. H. Churchill, D. J. Reilly, J. Xiang, C. M. Lieber, and C. M. Marcus, Nat. Nanotechnol. **2**, 622 (2007).
[24]J. M. Elzerman, R. Hanson, L. H. W. van Beveren, B. Witkamp, L. M. K. Vandersypen, and L. P. Kouwenhoven, Nature (London) **430**, 431 (2004).
[25]J. R. Petta, A. C. Johnson, J. M. Taylor, E. A. Laird, A. Yacoby, M. D. Lukin, C. M. Marcus, M. P. Hanson, and A. C. Gossard, Science **309**, 2180 (2005).
[26]F. H. L. Koppens, C. Buizert, K. J. Tielrooij, I. T. Vink, K. C. Nowack, T. Meunier, L. P. Kouwenhoven, and L. M. K. Vandersypen, Nature (London) **442**, 766 (2006).
[27]R. Hanson, L. P. Kouwenhoven, J. R. Petta, S. Tarucha, and L. M. K. Vandersypen, Rev. Mod. Phys. **79**, 1217 (2007).
[28]N. Shaji, C. B. Simmons, M. Thalakulam, L. J. Klein, H. Qin, H. Luo, D. E. Savage, M. G. Lagally, A. J. Rimberg, R. Joynt, M. Friesen, R. H. Blick, S. N. Coppersmith, and M. A. Eriksson, e-print arXiv:0708.0794.